

---

# A Near-Optimal Hierarchical Estimate Based Adaptive Finite Element Method for Obstacle Problems

Qingsong Zou

Department of Scientific Computing and Computer Applications, Sun Yat-sen University,  
Guangzhou 510275, P. R. China, mcszqs@mail.sysu.edu.cn

## 1 Introduction

In this paper, we will derive a novel adaptive finite element method for the following symmetric, elliptic obstacle problem: Find  $u \in K$  such that

$$a(u, v - u) \geq (f, v - u) \quad \forall v \in K \quad (1)$$

where  $\Omega \subset \mathbb{R}^2$  is a bounded polygonal domain with Lipschitz-continuous boundary  $\partial\Omega$ ,  $\psi \in C(\overline{\Omega})$  is a lower obstacle satisfying  $\psi \leq 0$  on  $\partial\Omega$ ,  $f \in L^2(\Omega)$  is a load term and

$$K = \{v \in H_0^1(\Omega) \mid v \geq \psi \text{ a.e. in } \Omega\},$$

and

$$a(v, w) = \int_{\Omega} \nabla v \cdot \nabla w, \quad v, w \in H_0^1(\Omega).$$

This problem admits a unique solution  $u$  since  $K$  is a nonempty, closed, and convex set, and  $a(\cdot, \cdot)$  is  $H_0^1(\Omega)$ -coercive.

Adaptive solvers are now widely used in numerical simulations of lots of problems for better accuracy with minimal computational cost. The reasons for choosing adaptive method for the problem (1) are two-folded. First, the grid in the contact zone is often not necessarily as fine as that in the non-contact zone. Secondly, the solution  $u$  may have singularity in some local areas. Therefore, for obstacle problems, a finite element solution on a suitable non-uniform grid may approximate the exact solution much better than that on a uniform grid with the same number of *degrees of freedoms*. Solvers which can generate non-uniform grids adaptively according to the *problem to-be-solved* are desired.

The adaptive solver in this paper will be established based on a *near-optimal* hierarchical estimate. Note that the hierarchical a posteriori analysis can be traced back to the pioneering works [2, 7, 20] and the monographs [1, 19]. The hierarchical analysis for obstacle problems have been studied in [13, 18, 22]. The hierarchical estimate presented in this paper improves the results in [22] by estimating directly

the energy norm of the discretization error, instead of the energy functional of the discretization error in [22].

This paper is organized as follows. In Sect. 2, we present a *near-optimal* hierarchical estimate for obstacle problems. A detailed description of our adaptive method will be presented in Sect. 3. In Sect. 4, numerical experiments will be given to show that our algorithm has the optimal convergence rate.

Throughout this paper, “ $A \lesssim B$ ” means that  $A$  can be bounded by  $B$  multiplied with a generic constant depending only on the shape regularity of the underlying grid, “ $A \simeq B$ ” means “ $A \lesssim B$ ” and “ $B \lesssim A$ ”.

## 2 A Near-Optimal Hierarchical Error Estimate

Let  $\mathcal{T}$  be a conforming and shape regular triangulation of  $\Omega$  with  $\mathcal{N}$  and let  $\mathcal{E}$  denote the set of all vertices and interior edges, respectively. We introduce the space  $\mathcal{S} \subset H_0^1(\Omega)$  of piecewise linear finite elements on  $\mathcal{T}$  spanned by the nodal basis  $\{\phi_p \mid p \in \mathcal{N} \cap \Omega\}$ . The finite element discretization of (1) reads as

$$u_{\mathcal{S}} \in K_{\mathcal{S}} : \quad a(u_{\mathcal{S}}, v - u_{\mathcal{S}}) \geq (f, v - u_{\mathcal{S}}) \quad \forall v \in K_{\mathcal{S}} \quad (2)$$

where the discrete constraints set

$$K_{\mathcal{S}} = \{v \in \mathcal{S} \mid v(p) \geq \psi(p) \quad \forall p \in \mathcal{N}\}.$$

Note that  $K_{\mathcal{S}} \subset K$ , if  $\psi \in \mathcal{S}$ .

We define the *residual type* functional  $\sigma_{\mathcal{S}}$  by

$$\langle \sigma_{\mathcal{S}}, v \rangle = (f, v) - a(u_{\mathcal{S}}, v) = \int_{\Omega} f v + \sum_{E \in \mathcal{E}} \int_E j_E v, \quad \forall v \in H_0^1(\Omega)$$

where  $j_E = \partial_{\mathbf{n}} u_{\mathcal{S}}|_{\tau_2} - \partial_{\mathbf{n}} u_{\mathcal{S}}|_{\tau_1}$  denotes the jump of the normal flux across the common edge  $E = \tau_1 \cap \tau_2$  of two triangles  $\tau_1, \tau_2 \in \mathcal{T}$  and  $\mathbf{n}$  denotes the normal vector on  $E$  pointing from  $\tau_1$  to  $\tau_2$ . For all  $E \in \mathcal{E}$ , let  $\phi_E$  be the piecewise affine function characterized by  $\phi_E(p) = \delta_{x_E, p}$  for all  $p \in \mathcal{N}' = \mathcal{N} \cup \{x_{E'} \mid E' \in \mathcal{E}\}$ , here  $x_{E'}$  is the midpoint of  $E'$ . We define

$$\rho_E = \langle \sigma_{\mathcal{S}}, \phi_E \rangle \|\phi_E\|^{-1}, \quad E \in \mathcal{E}$$

and will use  $|\rho_E|$  as our error indicators. Note that the similar edge-oriented indicators have been introduced in the hierarchical estimate for variational equations [2, 5], and for variational inequalities [11, 13, 18, 22]. Not all the  $\rho_E, E \in \mathcal{E}$  are efficient. To determine the efficient  $\rho_E$ , we let

$$\mathcal{N}^{\bullet} = \{p \in \mathcal{N} \mid u_{\mathcal{S}}(p) = \psi(p) \text{ or } p \in \partial\Omega\}, \quad \mathcal{N}^{\circ} = \{p \in \mathcal{N} \cap \Omega \mid u_{\mathcal{S}}(p) > \psi(p)\}$$

respectively be the set of contact and non-contact nodes and

$$\mathcal{E}^\bullet = \{E \in \mathcal{E} | \mathcal{N}_E \subset \mathcal{N}^\bullet\}, \quad \mathcal{E}^\circ = \{E \in \mathcal{E} | \mathcal{N}_E \cap \mathcal{N}^\circ \neq \emptyset\}$$

be the set of contact and non-contact edges, where  $\mathcal{N}_E = \mathcal{N} \cap E$  be the nodes on  $E$ ,  $E \in \mathcal{E}$ . Moreover we define  $\mathcal{E}^+ := \{E \in \mathcal{E} | \rho_E \geq 0\}$  and let

$$\mathcal{E}_1 = \mathcal{E} \setminus \mathcal{E}_2, \quad \mathcal{E}_2 = \mathcal{E}^\circ \cup \mathcal{E}^+.$$

The indicators  $|\rho_E|$ ,  $E \in \mathcal{E}_2$  are efficient.

The second type of indicators are patch-oriented quantities  $\rho_p = \|h_p f\|_{0,\omega_p}$ ,  $p \in \mathcal{N}$ , where the patch  $\omega_p = \text{supp } \phi_p$ . We define

$$\mathcal{N}_2 = \{p \in \mathcal{N} | f_p \geq 0\} \cup \mathcal{N}^\circ.$$

The indicators  $\rho_p$  are efficient for all  $p \in \mathcal{N}_2$ .

To present efficiency and reliability of our hierarchial estimator, we need to split again the set of contact nodes  $\mathcal{N}^\bullet$  into

$$\mathcal{N}^\bullet = \mathcal{N}_0^\bullet \cup \mathcal{N}_1^\bullet \cup \mathcal{N}_2^\bullet \cup \mathcal{N}_3^\bullet \cup \mathcal{N}_4^\bullet$$

where

$$\mathcal{N}_0^\bullet = \{p \in \mathcal{N}^\bullet \mid u_S|_{\omega_p} = \psi|_{\omega_p}, f|_{\omega_p} \leq 0, j_E \leq 0 \forall E \in \mathcal{E}_p\}$$

is the set of the so-called *full-contact* nodes (c.f., [10, 18]) and

$$\mathcal{N}_1^\bullet = \{p \in \mathcal{N}^\bullet \mid u_S|_{\omega_p} = \psi|_{\omega_p}, f_p \leq 0, j_E \leq 0 \forall E \in \mathcal{E}_p\} \setminus \mathcal{N}_0^\bullet,$$

$$\mathcal{N}_2^\bullet = \{p \in \mathcal{N}^\bullet \mid u_S|_{\omega_p} = \psi|_{\omega_p}, f_p \leq 0, \exists E \in \mathcal{E}_p \text{ s.t. } j_E > 0\},$$

$$\mathcal{N}_3^\bullet = \{p \in \mathcal{N}^\bullet \mid u_S > \psi \text{ in } \omega_p \setminus \{p\}\}, \mathcal{N}_4^\bullet = \mathcal{N}^\bullet \setminus (\mathcal{N}_0^\bullet \cup \mathcal{N}_1^\bullet \cup \mathcal{N}_2^\bullet \cup \mathcal{N}_3^\bullet).$$

We define our hierarchical estimator by

$$\eta^2 = \sum_{E \in \mathcal{E}_2} \rho_E^2 + \sum_{p \in \mathcal{N}_3^\bullet \cup \mathcal{N}_4^\bullet} \|h_p f\|_{0,\omega_p}^2$$

and the oscillation by

$$\text{osc}^2 = \sum_{p \in \mathcal{N} \setminus \mathcal{N}_0^\bullet} \text{osc}_p^2 + \sum_{p \in \mathcal{N}_3^\bullet} \|\nabla(\psi - u_S)\|_{0,\omega_p}^2$$

where the patch-oriented oscillation (c.f., [9]) is defined for all  $p \in \mathcal{N}$  by

$$\text{osc}_p = \|h_p(f - f_p)\|_{0,\omega_p}.$$

Here  $f_p = 0$  if  $p \in \mathcal{N}_2^\bullet$  and  $f_p = \frac{1}{|\omega_p|} \int_{\omega_p} f$  otherwise. Note that the oscillation defined above is smaller than that defined in [22] and it seems to be really of *high-order*.

We have the following efficiency and reliability results.

**Theorem 1.** *There holds the lower bound*

$$\eta \lesssim \|e\| + osc. \quad (3)$$

Moreover, if  $\psi \in \mathcal{S}$ , there holds the upper bound

$$\|e\| \lesssim \eta + osc. \quad (4)$$

Note that in the above theorem, the efficiency result holds for general obstacle  $\psi \in C(\overline{\Omega})$  but the reliability result only holds for obstacle functions which are piecewise affine with respect to the underlying grid  $\mathcal{T}$ . The detailed and very complicated proof of this theorem will be given in a future paper [21].

### 3 An Adaptive Finite Element Method

This section is dedicated to the presentation of an adaptive finite element method for the obstacle problem (1).

The main purpose of our adaptive algorithm is to construct the sequence of triangulations  $\mathcal{T}_j$ ,  $j = 0, 1, 2, \dots$ , resulting from the  $j$ th local refinement steps of an initial triangulation  $\mathcal{T}_0$ . Here and throughout the paper, the subscript  $j$  will always refer to the corresponding triangulation  $\mathcal{T}_j$  as, for example, in  $\mathcal{N}_j$ ,  $\mathcal{E}_j$ ,  $\mathcal{S}_j$ ,  $u_j$ ,  $\psi_j$ , and so on.

As a standard adaptive scheme, our adaptive algorithm consists of loops of the following four basic steps

$$Solve \rightarrow Estimate \rightarrow Mark \rightarrow Refine.$$

which will be described in the following.

**Solve.** To solve the discrete problem (2), we apply *monotone multigrid methods* proposed in [12] on the non-uniform grid  $\mathcal{T}_j$ . Our numerical implementation shows that even for non-uniform grid, this monotone multigrid method requires only  $O(n_j)$  operations for each iteration, where  $n_j$  denotes the degree of freedoms of  $\mathcal{T}_j$ , and it converges more rapidly than the standard nonlinear Gauss–Seidel method since its convergence rate is about 1.

Given a mesh  $\mathcal{T}_j$  and an initial iterate  $u_j^0$  for the solution, the algorithm **SOLVE** computes the discrete solution

$$u_j := \text{SOLVE}(\mathcal{T}_j, u_j^0).$$

**Estimate.** We use the hierarchical estimators presented in the previous section to estimate the error. For a given mesh  $\mathcal{T}_j$  and the finite element approximation  $u_j$ , the subroutine **ESTIMATE** computes the edgewise hierarchical indicators  $\rho_E$  for all edges  $E \in \mathcal{E}_{j2}$  and the nodalwise indicators  $\rho_p$  for all  $p \in \mathcal{N}_{j3}^\bullet \cup \mathcal{N}_{j4}^\bullet$ :

$$(\{\rho_E\}_{E \in \mathcal{E}_{j2}}, \{\rho_p\}_{p \in \mathcal{N}_{j3}^\bullet \cup \mathcal{N}_{j4}^\bullet}) = \text{ESTIMATE}(\mathcal{T}_j, u_j).$$

**Mark.** We use a variant of Dörfler marking strategy [8] described as below. First, we order all the quantities  $\{|\rho_E|\}_{E \in \mathcal{E}_{j2}}$  and  $\{\rho_p\}_{p \in \mathcal{N}_{j3}^\bullet \cup \mathcal{N}_{j4}^\bullet}$  according to their size. Secondly, proceeding from the largest to smallest quantities, we collect all entries from these two sets until they sum up to  $\theta \eta_j$  where  $\theta \in (0, 1)$  is some given parameter. Finally, if  $\rho_E^2$  or  $\rho_p^2$  are contained in this collection, then all the triangles in the support of  $\phi_E$  or  $\phi_p$  are marked for refinement.

Given a mesh  $\mathcal{T}_j$  and the indicators  $(\{\rho_E\}_{E \in \mathcal{E}_{j2}}, \{\rho_p\}_{p \in \mathcal{N}_{j3}^\bullet \cup \mathcal{N}_{j4}^\bullet})$ , together with the parameter  $\theta$ , **MARK** generates a subset  $\tilde{\mathcal{T}}_j$  of  $\mathcal{T}_j$ :

$$\tilde{\mathcal{T}}_j = \mathbf{MARK}(\theta, \mathcal{T}_j, (\{\rho_E\}_{E \in \mathcal{E}_{j2}}, \{\rho_p\}_{p \in \mathcal{N}_{j3}^\bullet \cup \mathcal{N}_{j4}^\bullet})).$$

**Refine.** We will use the so-called *newest vertex bisection* techniques to refine the mesh  $\mathcal{T}_j$ : first we label one vertex of each triangle in  $\mathcal{T}_j$  as the *newest vertex*, the opposite edge of the newest vertex is called *reference edge*. After being labeled, each the element  $\tau \in \tilde{\mathcal{T}}_j$  is then bisected to two new children elements by connecting the newest vertex to the midpoint of the reference edge. After all the marked triangles are bisected, more bisections are necessary to eliminate the hanging nodes (cf., [3, 4, 15]). It is worth mentioning that here, each marked triangle is refined only once and consequently, the interior node property [14, 17] has been circumvented.

Given a mesh  $\mathcal{T}_j$  and a marked set  $\tilde{\mathcal{T}}_j$ , **REFINE** constructs the conforming and shape regular triangulation  $\mathcal{T}_{j+1}$ :

$$\mathcal{T}_{j+1} = \mathbf{REFINE}(\mathcal{T}_j, \tilde{\mathcal{T}}_j).$$

Now we are ready to present our adaptive finite element methods for (1) which consists of the loops of the above four subroutines **SOLVE**, **ESTIMATE**, **MARK**, and **REFINE**, consecutively. Given an initial triangulation  $\mathcal{T}_0$ , a tolerance  $\varepsilon > 0$  and a parameter  $0 < \theta < 1$ , our adaptive solver can be described as below:

$$u_{\text{FE}} = \mathbf{AFEM4OP}(\mathcal{T}_0, \varepsilon, \theta)$$

Set  $u_0 = 0$ , for  $j = 1, \dots$ , do the following:

1. Set  $u_j^0 = u_{j-1}$ , then  $u_j = \mathbf{SOLVE}(\mathcal{T}_j, u_j^0)$ .
2.  $(\{\rho_E\}_{E \in \mathcal{E}_{j2}}, \{\rho_p\}_{p \in \mathcal{N}_{j3}^\bullet \cup \mathcal{N}_{j4}^\bullet}) = \mathbf{ESTIMATE}(\mathcal{T}_j, u_j)$ .
3. Compute  $\eta_j$ . If  $\eta_j \leq \varepsilon$ ,  $u_{\text{FE}} = u_j$ , stop. Otherwise, go to Step 4.
4.  $\tilde{\mathcal{T}}_j = \mathbf{MARK}(\theta, \mathcal{T}_j, (\{\rho_E\}_{E \in \mathcal{E}_{j2}}, \{\rho_p\}_{p \in \mathcal{N}_{j3}^\bullet \cup \mathcal{N}_{j4}^\bullet}))$ .
5.  $\mathcal{T}_{j+1} = \mathbf{REFINE}(\mathcal{T}_j, \tilde{\mathcal{T}}_j)$ . Set  $j = j + 1$ , go to Step 1.

## 4 Numerical Experiments

In our numerical experiments, we will test two examples to verify if our algorithm **AFEM4OP** has a quasi-optimal convergence rate in terms of the number of degrees of freedom. Note that for adaptive finite element methods for elliptic PDEs, the optimal convergence rate has been obtained both theoretically and numerically in recent papers such as [6, 16, 17].

*Example 1* Constant Obstacle. Let the obstacle function  $\psi \equiv 0$ , the domain  $\Omega = (-1, 1)^2$ , and the radially symmetric right-hand side

$$f(x) = \begin{cases} -8r^2, & |x| > r \\ -8(2|x|^2 - r^2), & |x| \leq r \end{cases}.$$

This problem has the unique radially symmetric exact solution

$$u(x) = (\max\{r^2 - |x|^2, 0\})^2.$$

For simplicity, we select  $r = 0.7$  in our numerical computations. Then the circle  $\{x \in \Omega \mid r = 0.7\}$  is the free boundary of the problem which decompose the domain to the contact zone  $\{x \in \Omega \mid r > 0.7\}$  and the non-contact zone  $\{x \in \Omega \mid r < 0.7\}$ .

In our numerical experiments, the initial triangulation  $\mathcal{T}_0$  consisting of four congruent triangles. Selecting  $\theta = 0.5$  in **AFEM4OP**, we obtain the sequence of triangulations  $\mathcal{T}_j, j = 0, 1, \dots, 14$ . The left picture of Fig. 1 presents the discretization error

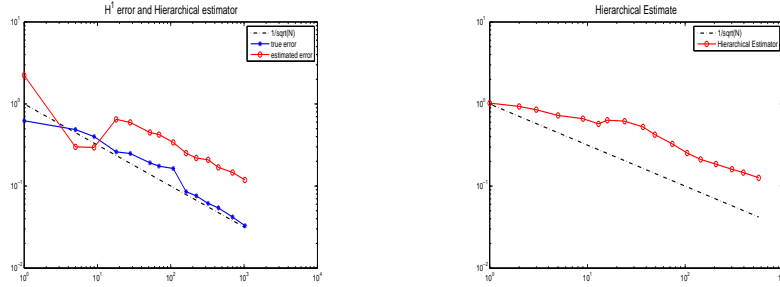


**Fig. 1.** *Left:* the exact error and the hierarchial estimator for Example 1, *Right:* the estimator for Example 2.

$\|u - u_{\mathcal{S}_j}\|$  and the hierarchical estimator  $\eta_j$  over the number  $n_j = \#\mathcal{T}_j$ . Obviously, both the exact error and the hierarchical estimator have an optimal convergence rate of  $\mathcal{O}(n_j^{-1/2})$ .

*Example 2* Lipschitz Obstacle. We consider (1) with  $\Omega = \{x \in \mathbb{R}^2 \mid |x_1| + |x_2| < 1\}$ , the right hand side  $f = -5$  and the Lipschitz obstacle

$$\psi(x) = -\text{dist}(x, \partial\Omega).$$

As in the first example, we apply the algorithm AFEM4OP to obtain a sequence of triangulations  $\mathcal{T}_j, j = 1, 2, \dots, 18$  based upon the initial triangulation  $\mathcal{T}_0$  consisting of four congruent triangles. The adaptive parameter  $\theta = 0.35$ . As no exact solution is available, the final approximate solution  $u_{18}$  is depicted in the left picture of Fig. 2 while the right picture shows the grid in the 18th iteration step. The

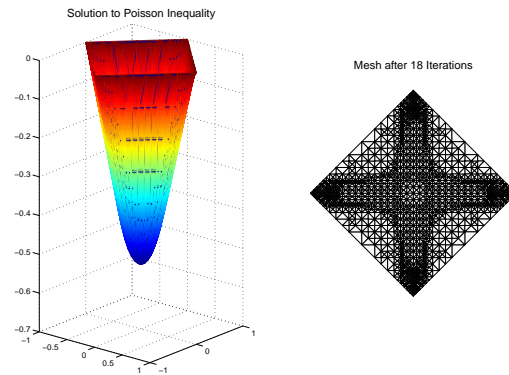


**Fig. 2.** Approximate solution  $u_{18}$  and the grid in the 18th adaptive iteration step.

triangulation is locally refined in the neighborhood of the free boundary which is in agreement with the corresponding lack of regularity. The hierarchical estimator is presented in the right picture of 1. We still observe that  $\eta_{T_j} = \mathcal{O}(n_j^{-1/2})$ .

## References

1. M. Ainsworth and J.T. Oden. *A Posteriori Error Estimation in Finite Element Analysis*. Wiley, New York, NY, 2000.
2. R.E. Bank and R.K. Smith. A posteriori error estimates based on hierarchical bases. *SIAM J. Numeric Anal.*, 30:921–935, 1993.
3. E. Bänsch. Local mesh refinement in 2 and 3 dimensions. *IMPACT Comput. Sci. Eng.*, 3: 181–191, 1991.
4. P. Binev, W. Dahmen, and R. DeVore. Adaptive finite element methods with convergence rates. *Numer. Math.*, 97(2):219–268, 2004.
5. F.A. Bornemann, B. Erdmann, and R. Kornhuber. A posteriori error estimates for elliptic problems in two and three space dimensions. *SIAM J. Numer. Anal.*, 33:1188–1204, 1996.
6. J.M. Cascon, C. Kreuzer, R.H. Nochetto, and K.G. Siebert. Quasi-optimal convergence rate for an adaptive finite element method. *SIAM J. Numer. Anal.*, 46(5):2524–2550, 2008.
7. P. Deuffhard, P. Leinen, and H. Yserentant. Concepts of an adaptive hierarchical finite element code. *IMPACT Comput. Sci. Eng.*, 1:3–35, 1989.
8. W. Dörfler. A convergent adaptive algorithm for Poisson’s equation. *SIAM J. Numer. Anal.*, 33:1106–1124, 1996.
9. W. Dörfler and R.H. Nochetto. Small data oscillation implies the saturation assumption. *Numer. Math.*, 91:1–12, 2002.
10. F. Fierro and A. Veiser. A posteriori error estimators for regularized total variation of characteristic functions. *SIAM J. Numer. Anal.*, 41(6):2032–2055 (electronic), 2003. ISSN 1095-7170.
11. R. Kornhuber. A posteriori error estimates for elliptic variational inequalities. *Comput. Math. Appl.*, 31:49–60, 1996.

12. R. Kornhuber. *Adaptive Monotone Multigrid Methods for Nonlinear Variational Problems*. Teubner, Stuttgart, 1997.
13. R. Kornhuber and Q. Zou. Efficient and reliable hierarchical error estimates for the discretization error of elliptic obstacle problems. *Math. Comput.*, in press, 2010.
14. K. Mekchay and R. Nochetto. Convergence of adaptive finite element methods for general second order linear elliptic PDE. *SIAM J. Numer. Anal.*, 43:1803–1827, 2005.
15. W.F. Mitchell. *Unified Multilevel Adaptive Finite Element Methods for Elliptic Problems*. PhD thesis, University of Illinois at Urbana-Champaign, 1988.
16. P. Morin, R.H. Nochetto, and K.G. Siebert. Data oscillation and convergence of adaptive fem. *SIAM J. Numer. Anal.*, 38:466–488, 2000.
17. P. Morin, R.H. Nochetto, and K.G. Siebert. Convergence of adaptive finite element methods. *SIAM Rev.*, 44:631–658, 2002.
18. K.G. Siebert and A. Veiser. A unilaterally constrained quadratic minimization with adaptive finite elements. *SIAM J. Optim.*, 18:260–289, 2007.
19. R. Verfürth. *A Review of a Posteriori Error Estimation and Adaptive Mesh-Refinement Techniques*. Wiley-Teubner, Chichester, 1996.
20. O.C. Zienkiewicz, J.P. De, S.R. Gago, and D.W. Kelly. The hierarchical concept in finite element analysis. *Comput. Struct.*, 16:53–65, 1983.
21. Q. Zou. A near-optimal hierarchical analysis for elliptic obstacle problems. *In preparation*.
22. Q. Zou, A. Veiser, R. Kornhuber, and C. Gräser. Hierarchical error estimates for the energy functional in obstacle problems. *Numer. Math.*, submitted, 2009.